Interconnected mean-field models: their dynamical repertoires

Najwa Moursli[1]

Internship Supervisors :

Pr. A.Destexhe[2], Ph.D. D.Depannmaecker[2], Ph.D. M.Carlu[2]

Pr. F.Villers[1] and Pr. X.Tannier[1]

Polytech-Sorbonne[1], UNIC-CNRS[2]

November 22, 2021

POLYTECH SORBONNE

cnrs

Table of contents

1 Motivations

Context

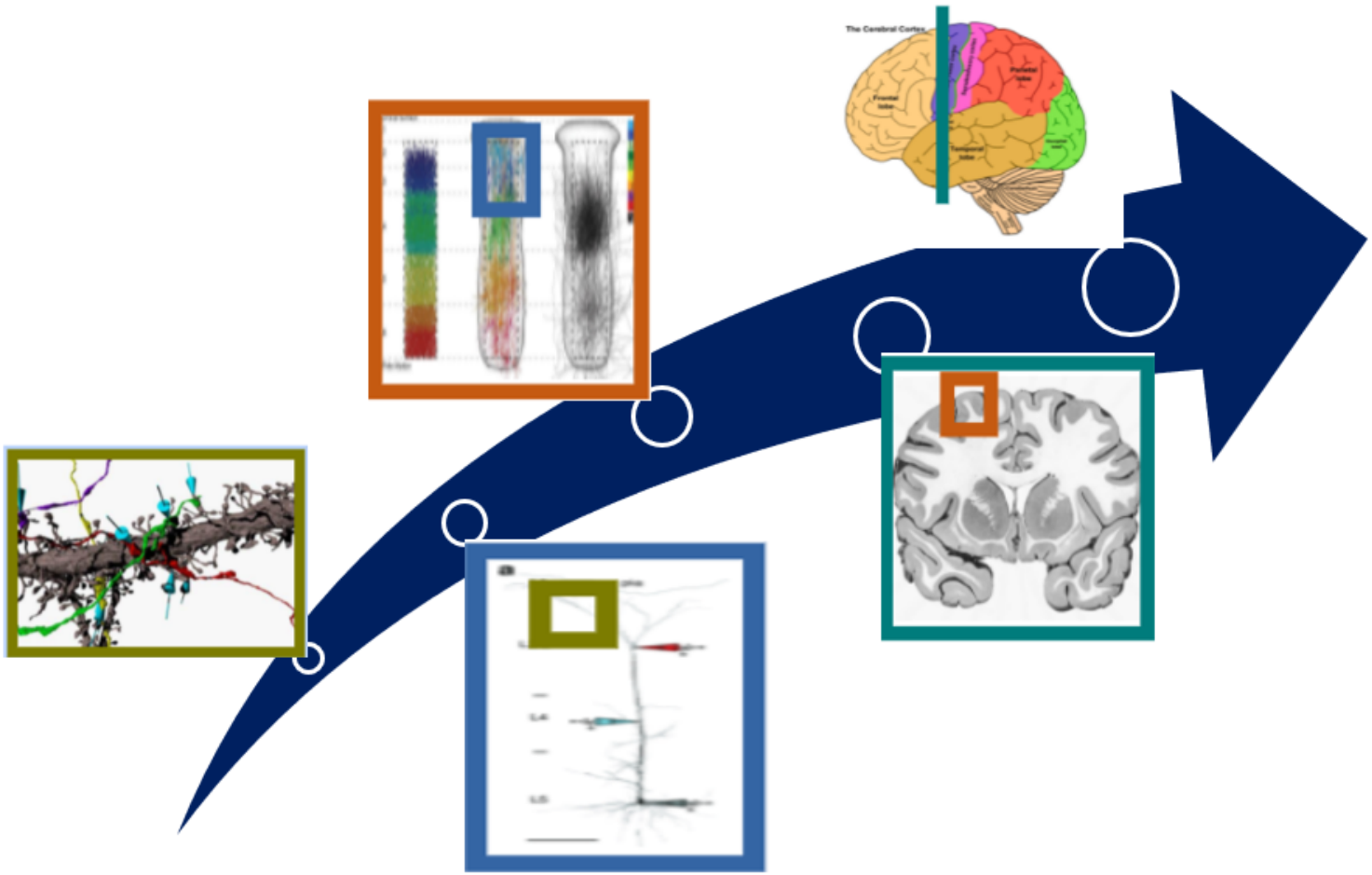

Figure 1: From single cells to the Connectome [1]

1 Motivations

Main Goals

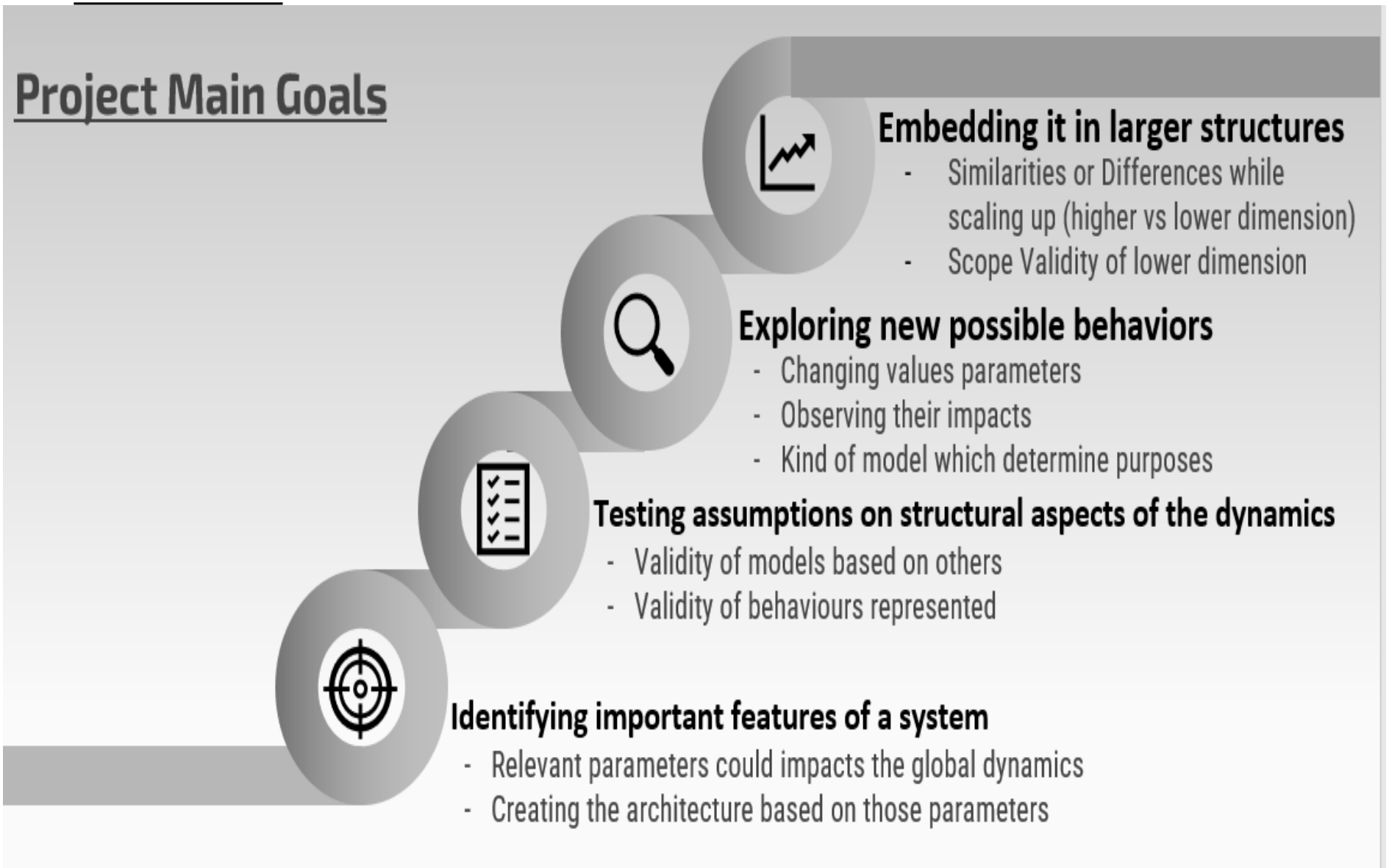

1 Motivations

Project Outline

Relevant model

Pinpoint relevant parameters to vary and model architecture to undergo simulation

Time varying Parameters

Simulate over the time of the chosen parameters and configuration model

State Mapping

Delimit different states observed to construct a bifurcation map

New dynamics

Resulting in the discover of new dynamics and behaviors to interpret

2 Fundamentals Concepts

Table of contents

Action Potential

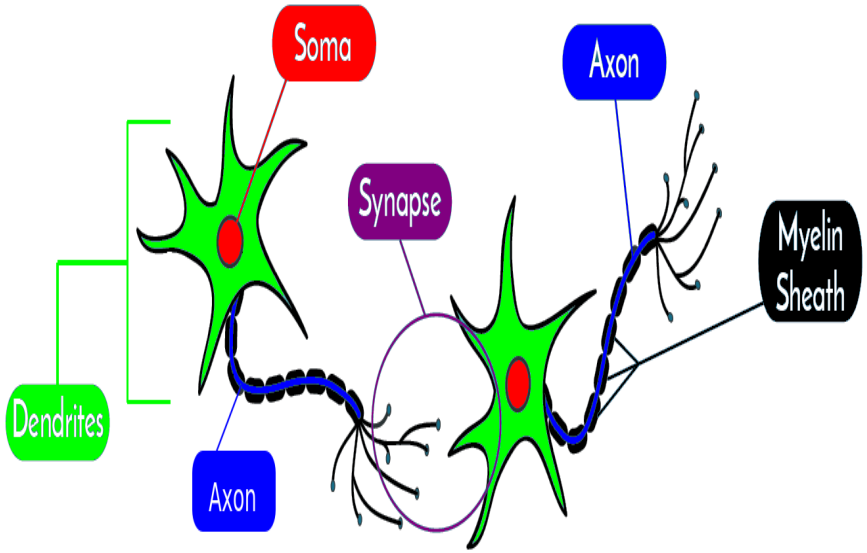

Figure 2: Representation of a single neuron

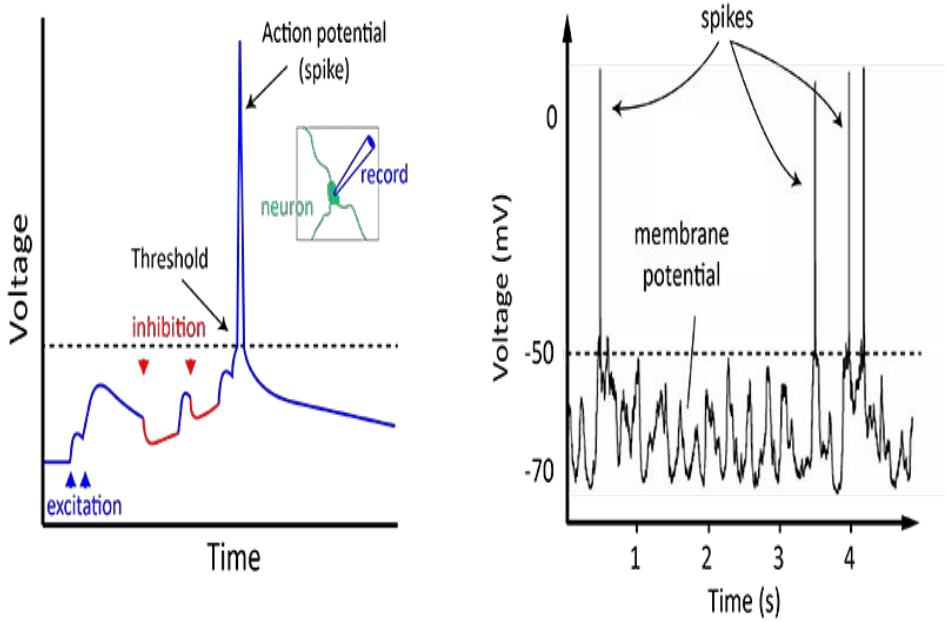

Figure 3: Action Potential Mechanism [2]

Neurons Types

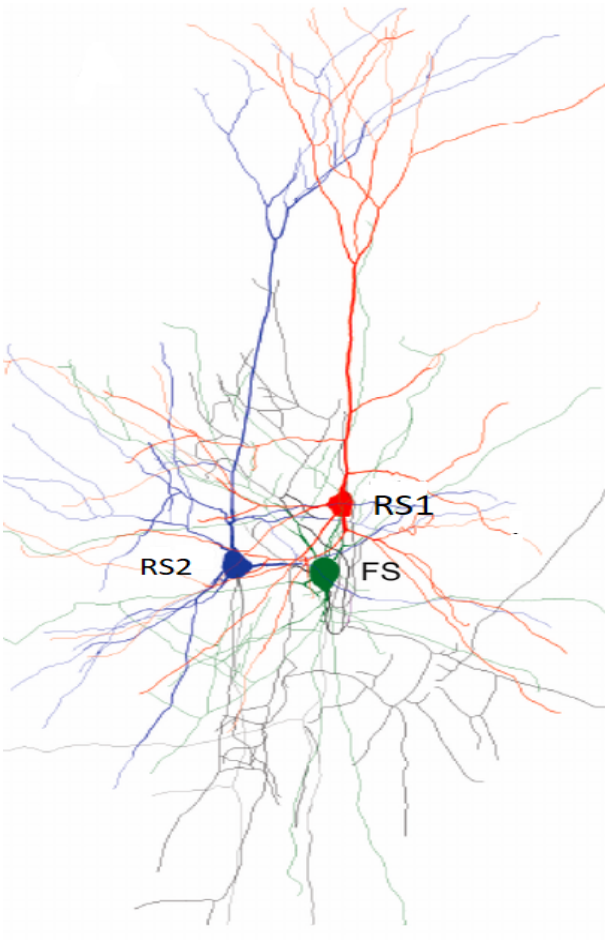

Figure 4: Connections of FS and RS cells [3]

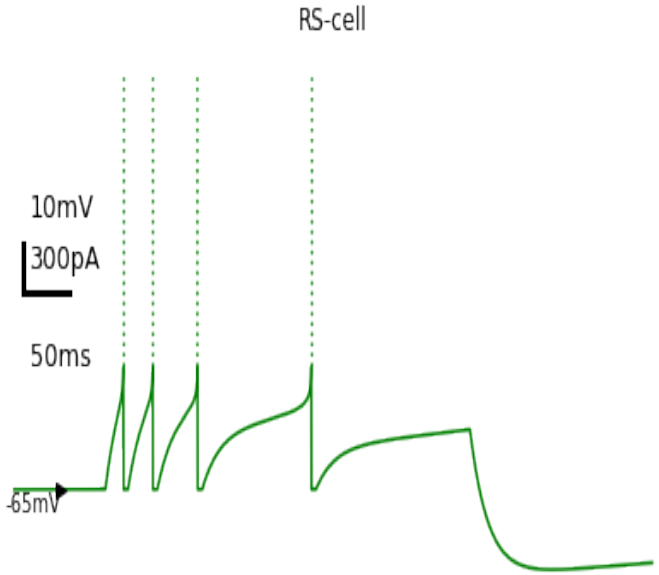

Figure 5: Firing pattern of RS cells [4]

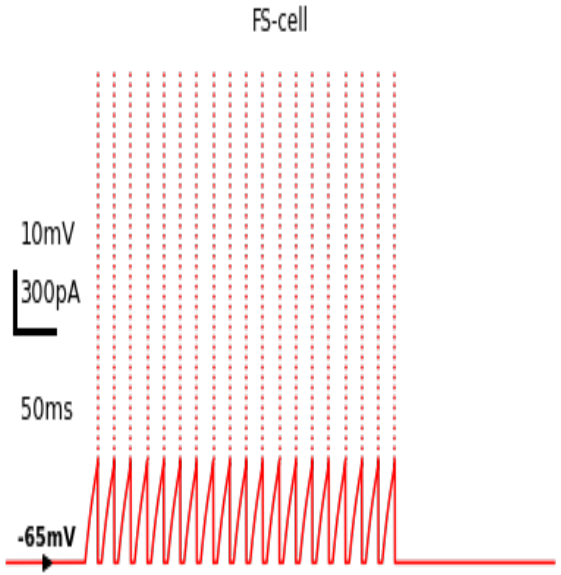

Figure 6: Firing pattern of FS cells [4]

Cortical columns

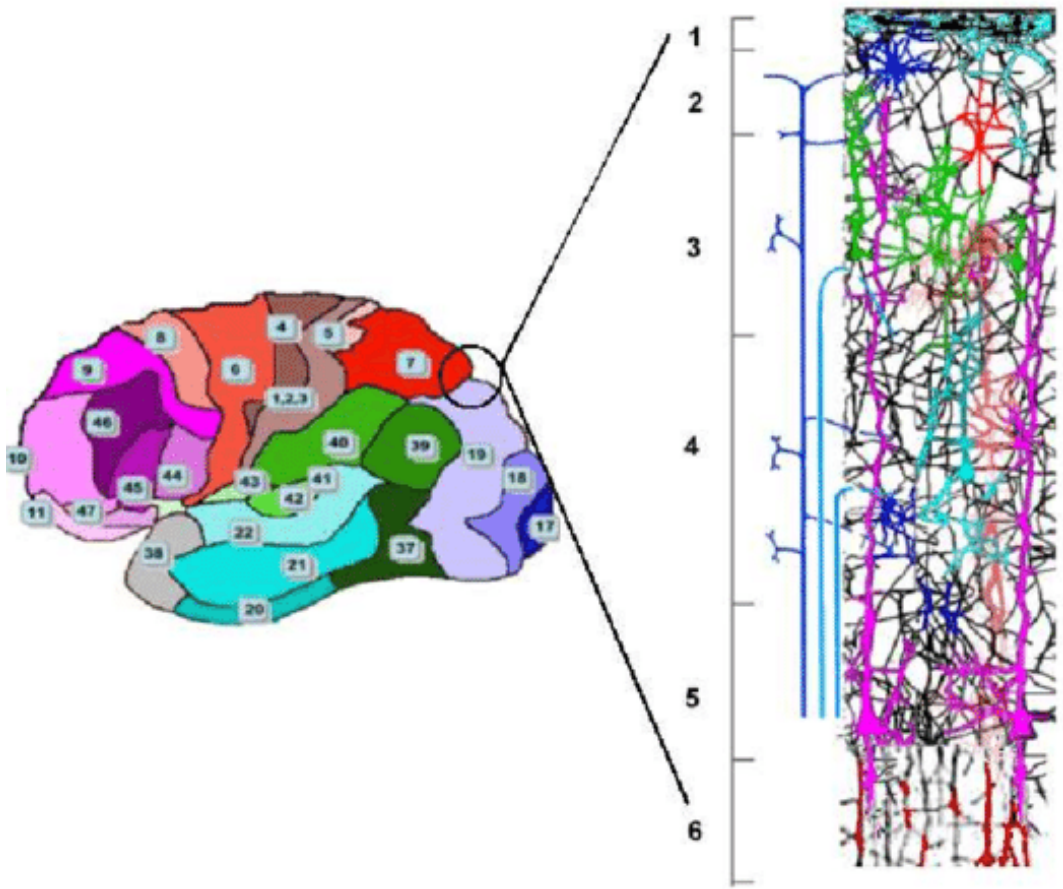

Figure 7: From cortex to column to simple circuit [5]

Brain States

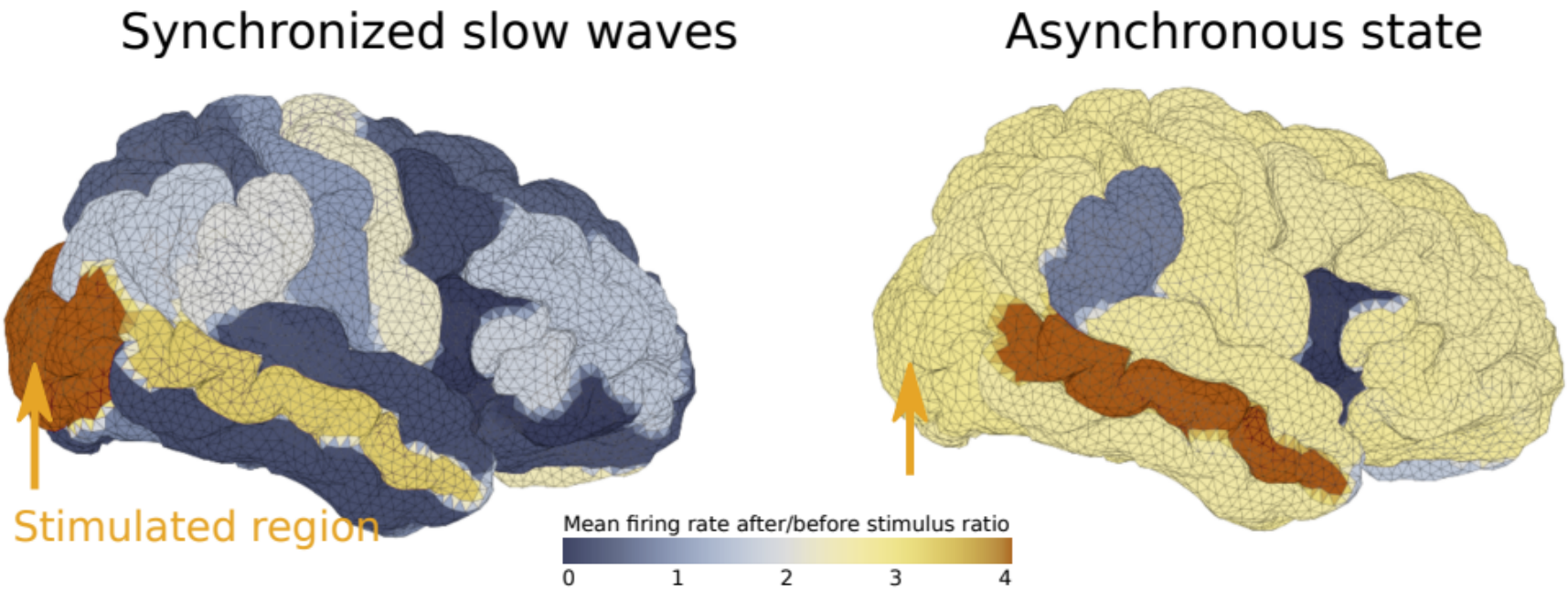

Figure 8: Mapping of synchronous vs asynchronous states for the whole-brain activity [1]

3 Methods

Table of contents

AdEx definition

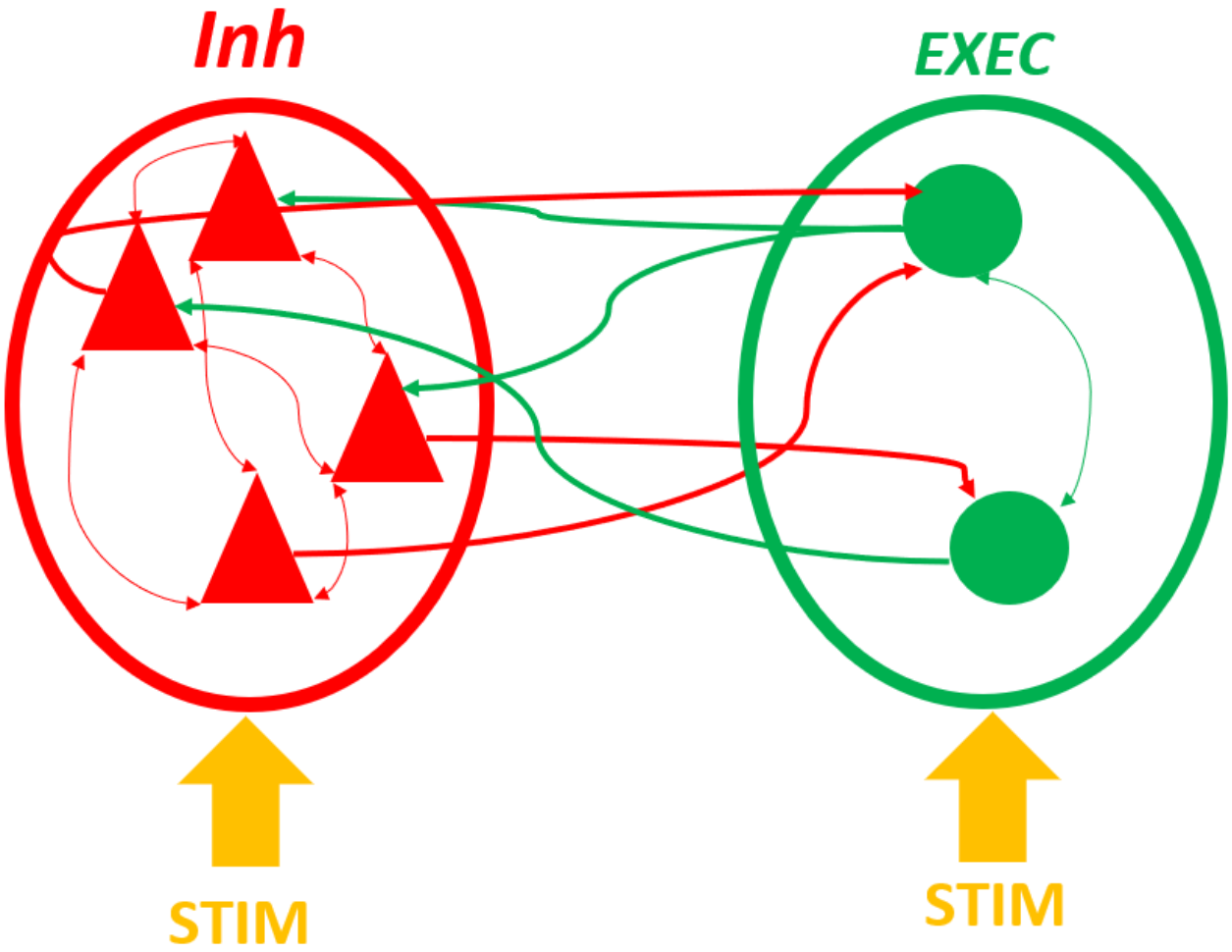

Figure 9: Schematic of the corresponding spiking AdEx neuron network with connections between and within both populations

AdEx Mathematical Formalism

AdEx characteristic equations :

$$\begin{cases} C_m \frac{d\nu}{dt} = -g_l(\nu - E_l) + gl * Dt * e^{\frac{w-\nu_t}{D_t}} - w + I_{syn}) \\ \tau_w \frac{dw}{dt} = a(\nu - E_L) - w \end{cases} \tag{1}$$

Synaptic equations:

$$\begin{cases} \frac{dG_{syn_{i,e}}}{dt} = -\frac{G_{syn_{i,e}}}{T_{syn}} \\ I_{syn} = -G_{syn_e} * (\nu - E_e) - G_{syn_i} * (\nu - E_i) \\ G_{syn_{i,e}}(t) = Q_{i,e} \sum_{i,e.pre} \mathcal{H}(t - t_{sp}^{e,i}(k)) \times e^{\frac{t - t_{sp}^{e,i}(k)}{\tau_{i,e}}} \end{cases} \tag{2}$$

Mean-field Definition

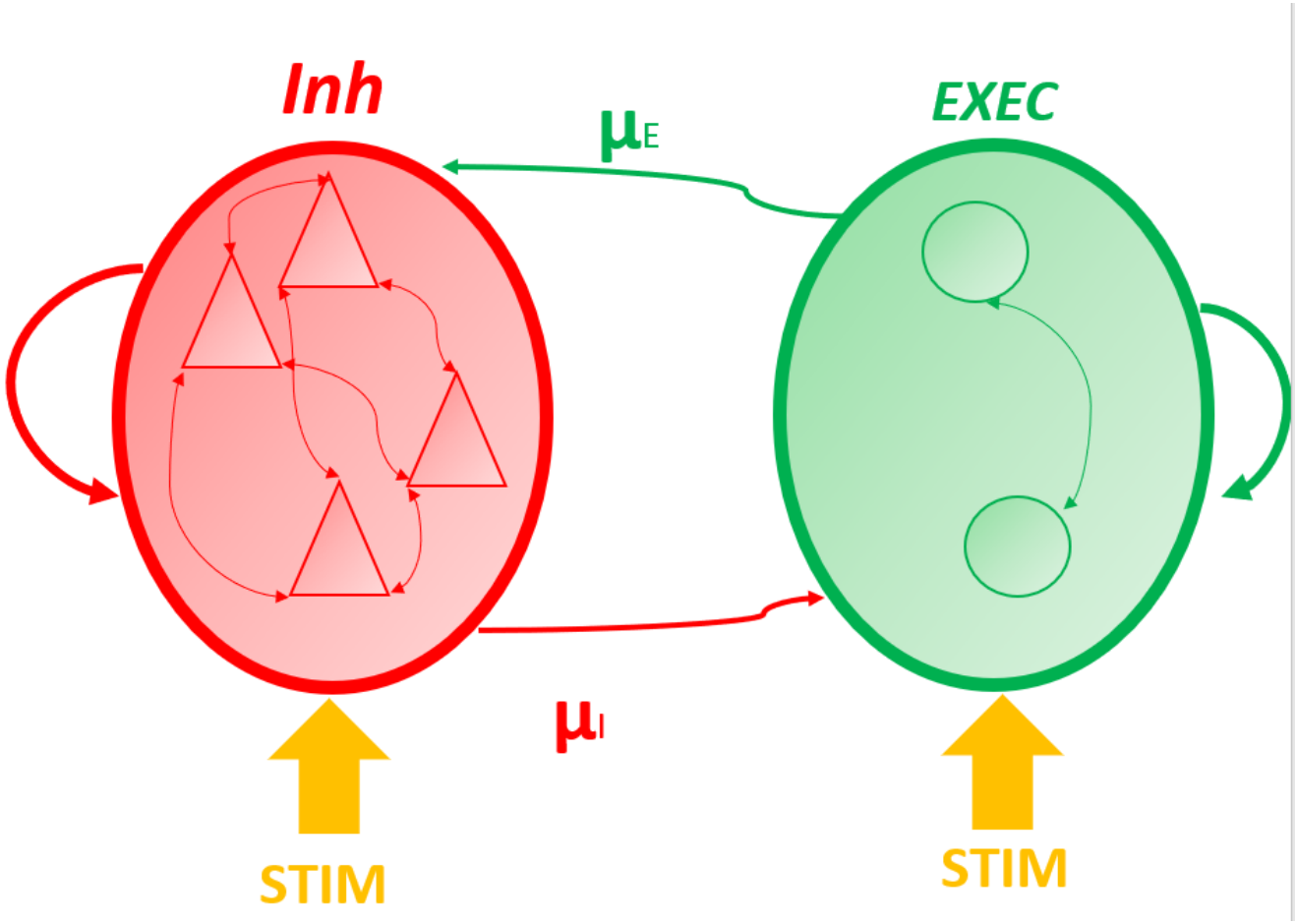

Figure 10: Mean-field neural mass model with synaptic feedforward and feedback connections. Each ellipse represents a population

Mean-Field Formalism

$$\mathbb{P}_T(E_\alpha|E'_\gamma) = \binom{N_\alpha}{\nu_\alpha N_\alpha T} \times \mathbb{P}_\alpha(E'_\gamma)^{(\nu_\alpha N_\alpha T)} \times (1-\mathbb{P}_\alpha(E'_\gamma))^{N_\alpha(1-\nu_\alpha N_\alpha T)} \quad (3)$$

$$W(\nu'|\nu) = \lim_{T\to 0} \frac{\prod_{\alpha=1,\dots,K} \mathbb{P}_T(E_\alpha|E'_\gamma)}{T} \quad (4)$$

$$\mathbb{P}_t(E'_\gamma) = \nu_\alpha(E'_\gamma) \times T \leq 1 \quad (5)$$

$$\Longrightarrow \partial_t \mathbb{P}_t(\nu) = \int_0^{\frac{1}{T}} \partial\nu' \times \mathbb{P}(\nu') \times W(\nu|\nu') - \mathbb{P}(\nu) \times W(\nu'|\nu) \quad (6)$$

$\partial\nu' \times \mathbb{P}(\nu') \times W(\nu|\nu')$ models the neurons flow entering in states E_α and $\mathbb{P}(\nu) \times W(\nu'|\nu)$, neurons flow leaving states E_α.

$$\begin{cases} T_{syn}\frac{d\nu_e(k)}{dt} &= F_e(\nu_e^{input}(k), \nu_i(k)) - \nu_e(k) \\ T_{syn}\frac{d\nu_i(k)}{dt} &= F_i(\nu_e^{input}(k), \nu_i(k)) - \nu_i(k) \\ \frac{dw(k)}{dt} &= \frac{-w(k)}{\tau_w * b * \nu_e(k)} + a(\mu_\nu(\nu_e(k), \nu_i(k), w(k)) - E_l) \end{cases} \quad (7)$$

Numerical Integration

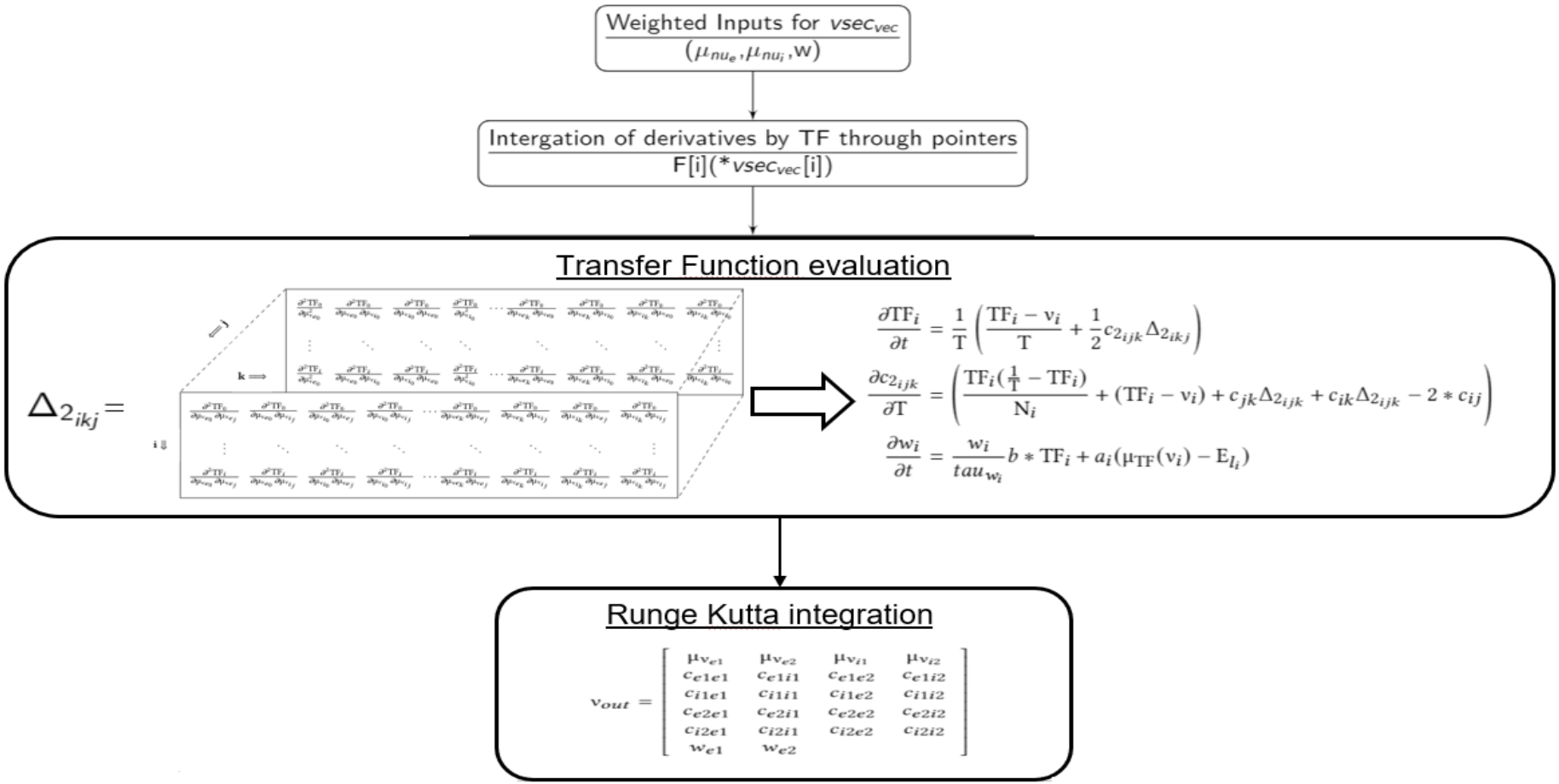

Figure 11: Transfer function as the key for in Mean-Field ODE integration

4 Simulations

Table of contents

One column

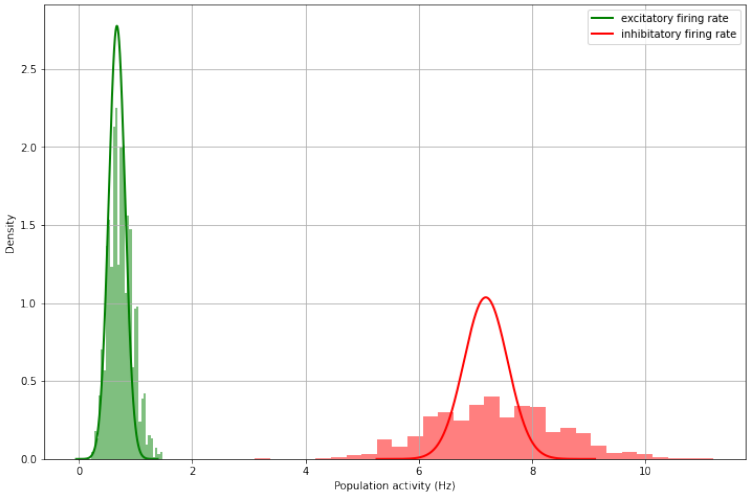

Figure 12: FR distribution sampled from the spiking simulation Gaussian predictions of the population activities

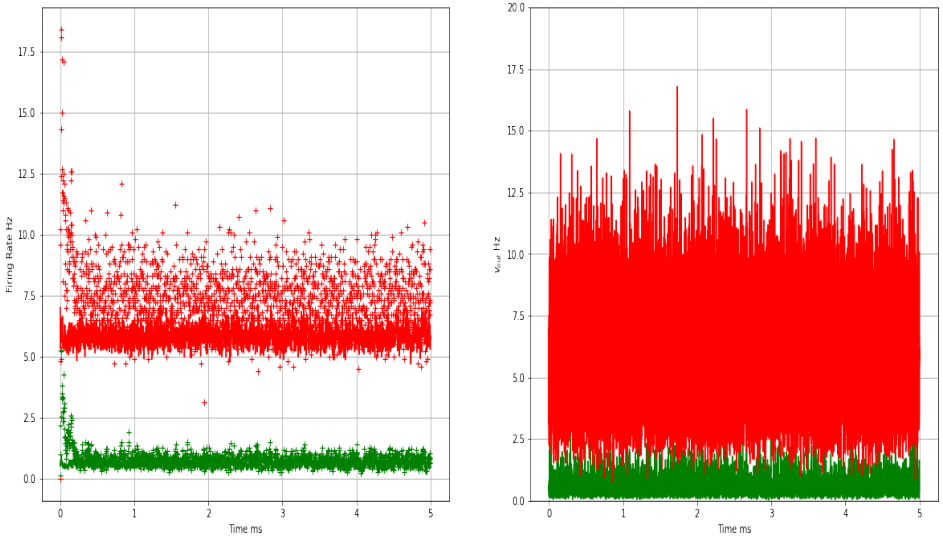

Figure 13: Time traces of the Firing rates and instantaneous transfer function of RS cells (+ is the MF prediction) and FS (+ is the MF prediction)

4 Simulations

Interconnected columns

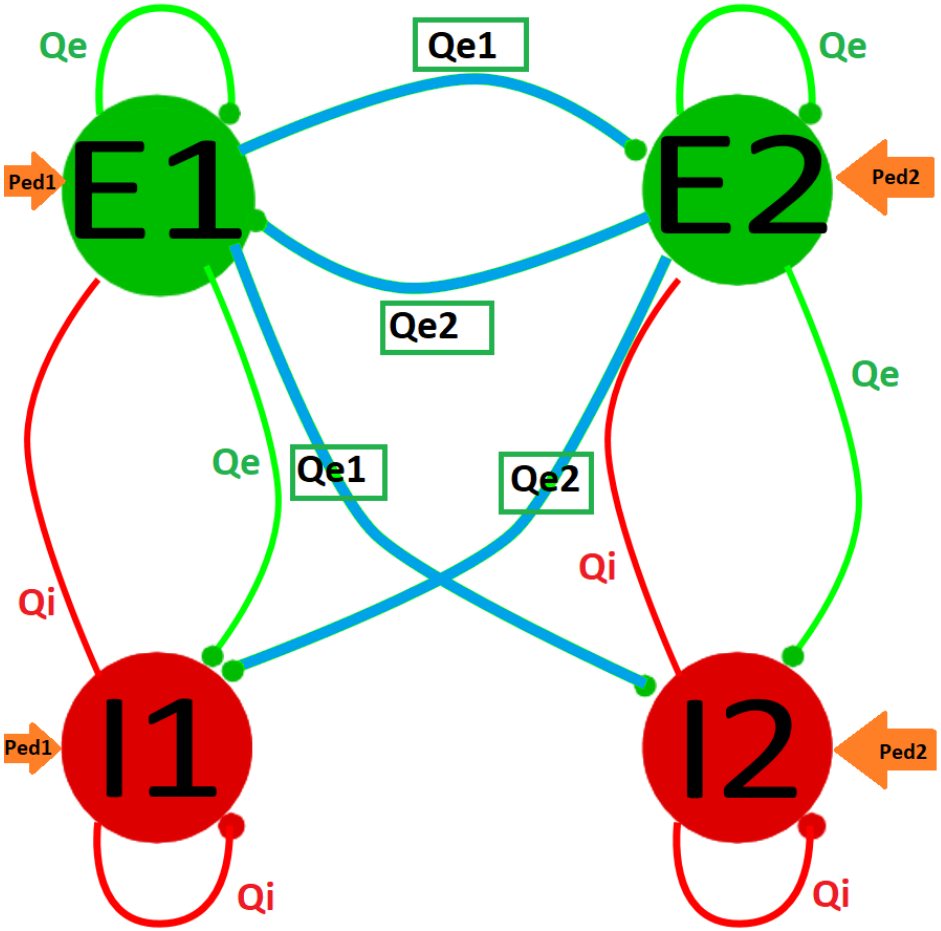

Figure 14: Configuration of the model : these connections are subject to a delay and each column receive a different external drive

j columns RECEIVE

i lines SEND

	E1	E2	I1	I2
E1	Qe	Qe_1	Qe	Qe_1
E2	Qe_2	Qe	Qe_2	Qe
I1	Qi	0	Qi	0
I2	0	Qi	0	Qi

Table 1: Synaptic weight connections matrix

j columns RECEIVE

i lines SEND

	E1	E2	I1	I2
E1	0	delay	0	delay
E2	delay	0	delay	0
I1	0	0	0	0
I2	0	0	0	0

Table 2: Synaptic connections delay matrix

Population E1 & E2

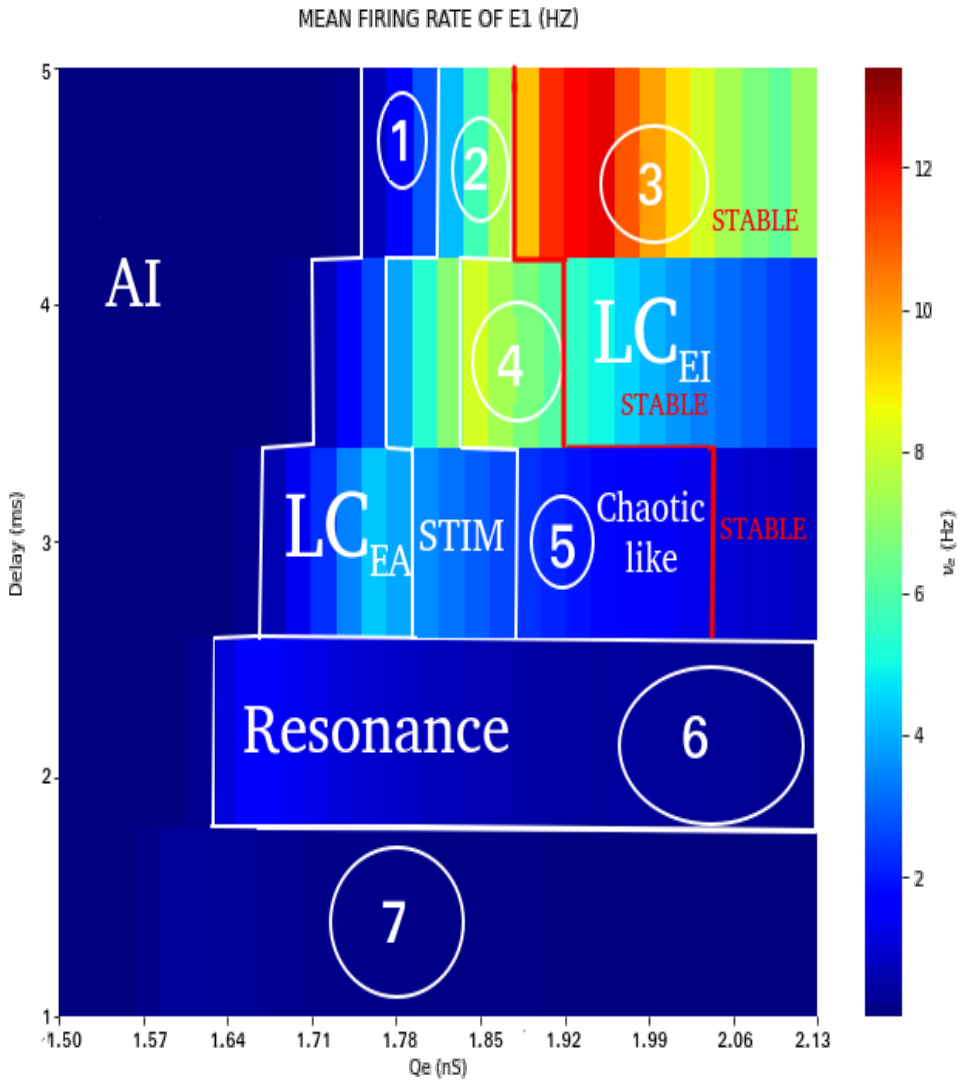

Figure 15: Bifurcation map of E1 states

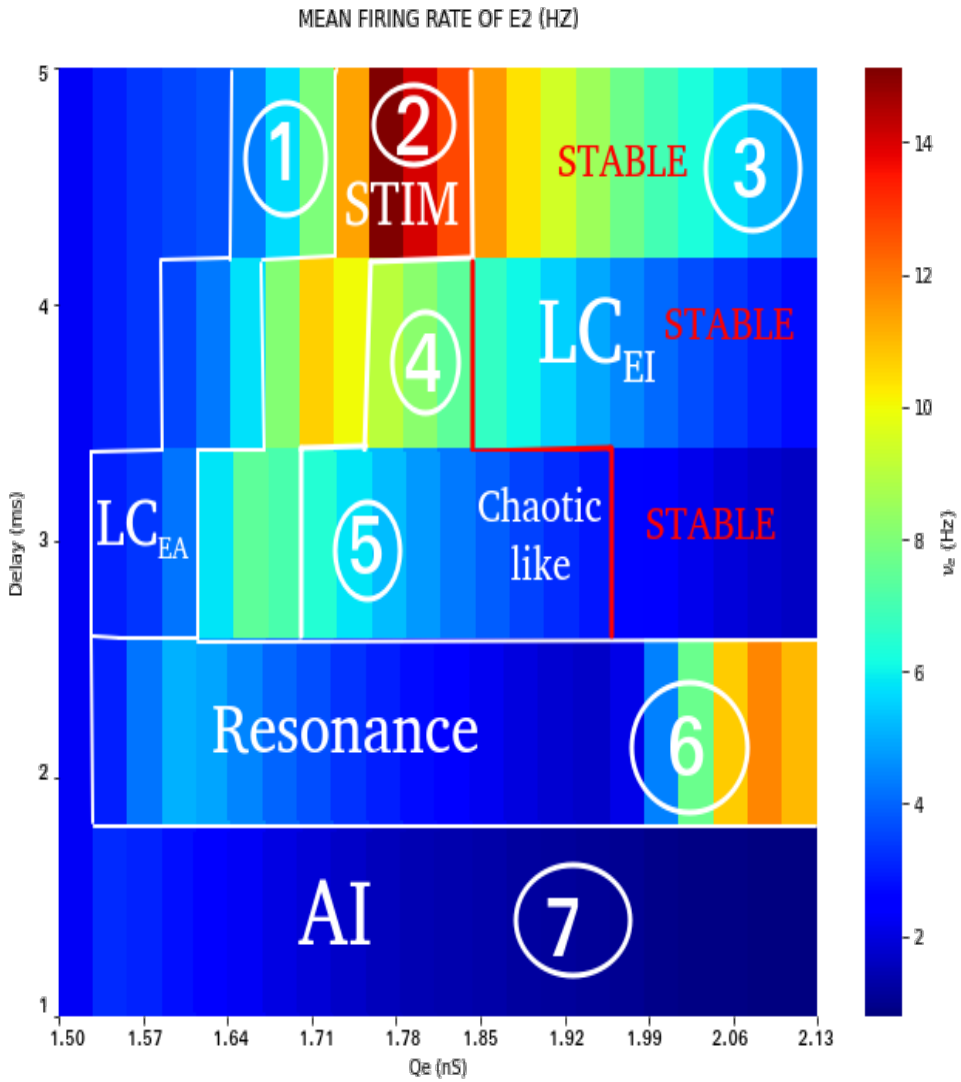

Figure 16: Bifurcation map of E2 states

Simulation results

	State 1 : LC_{EA}	State 2: Stimuli
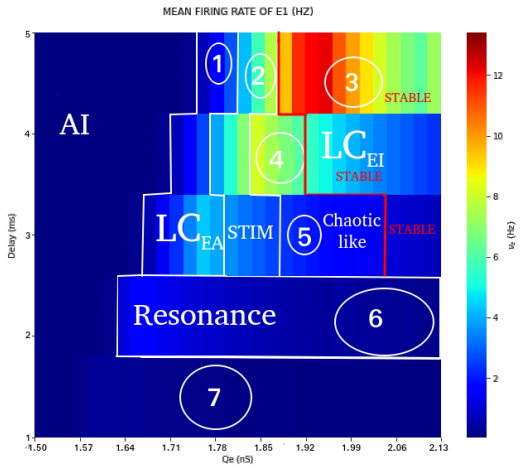	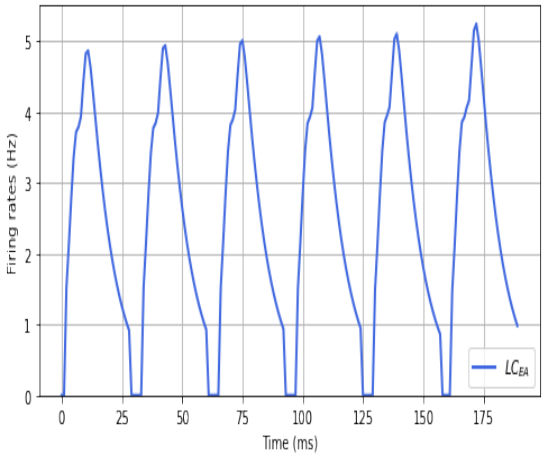	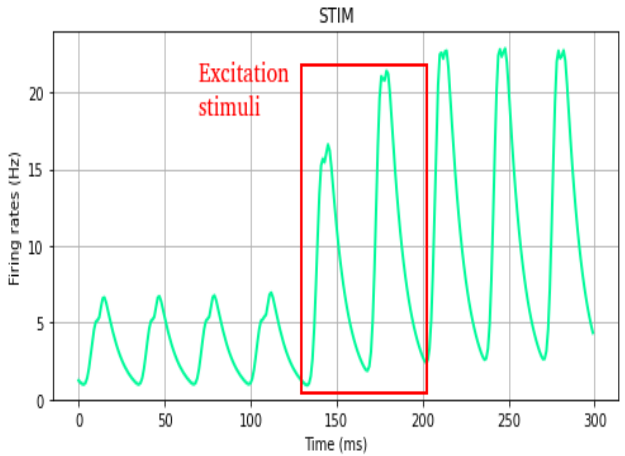
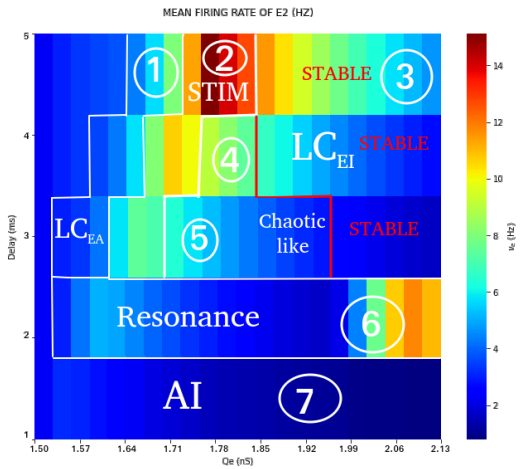	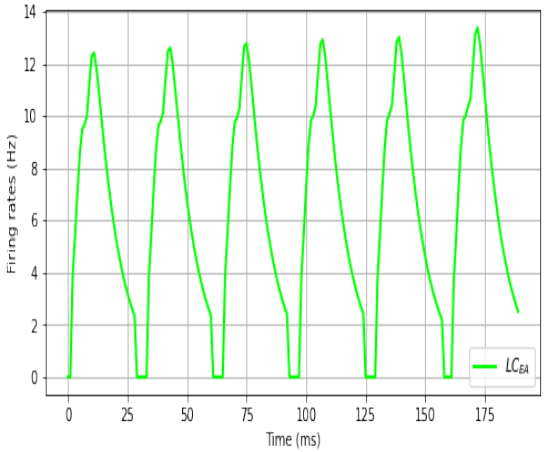	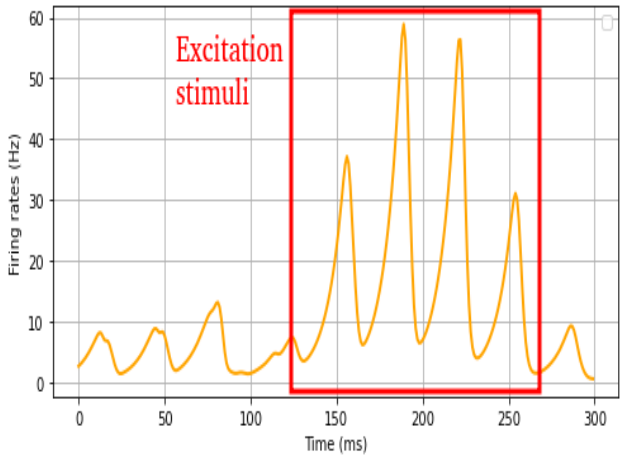

Simulation results

State 3 : Stable LC_{EI}

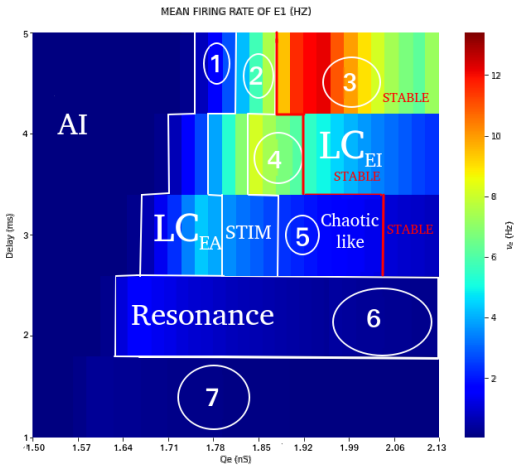

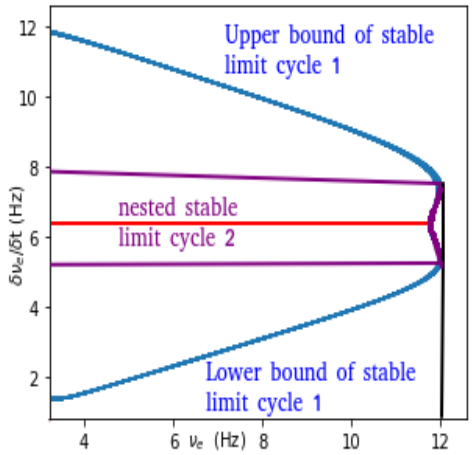

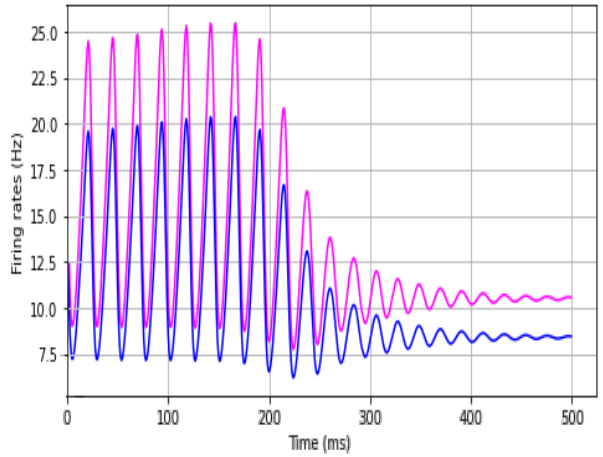

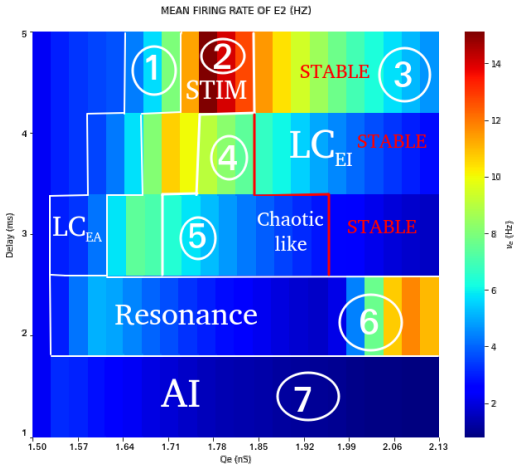

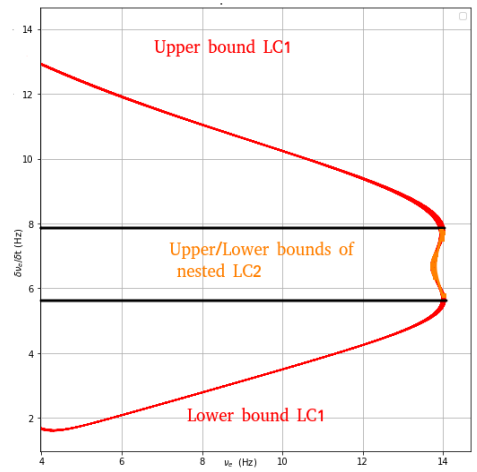

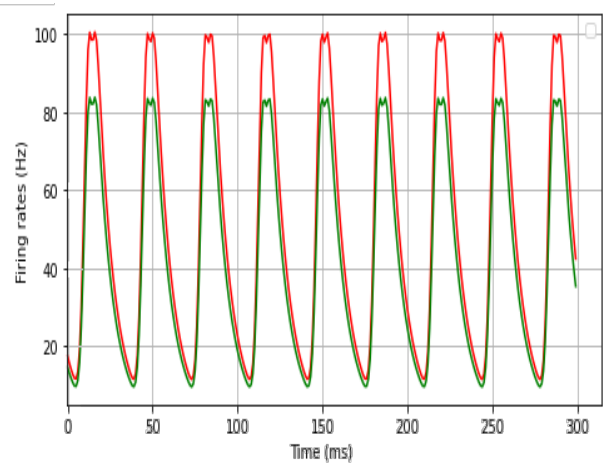

Simulation results

State 4 : Chaotic-like $State_1$

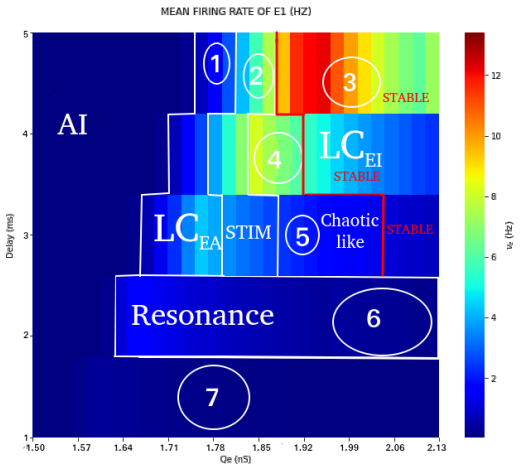

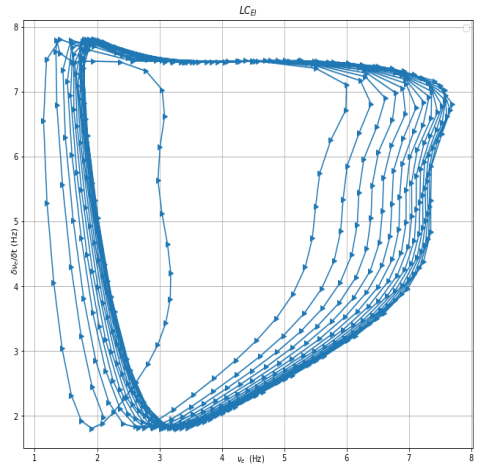

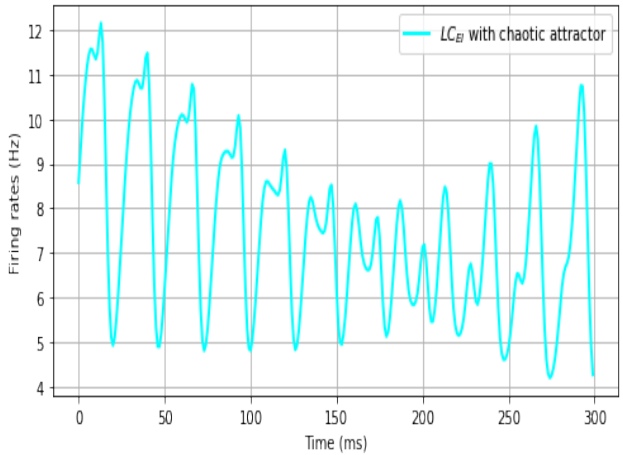

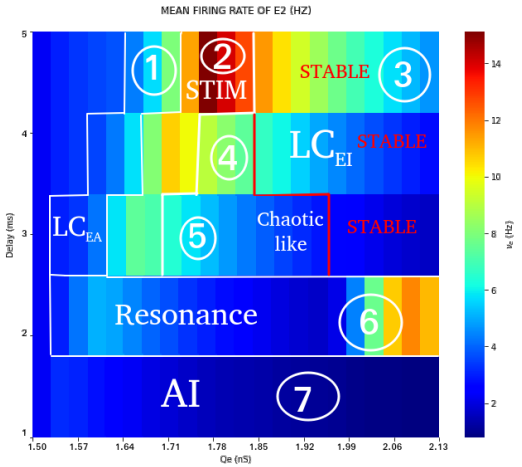

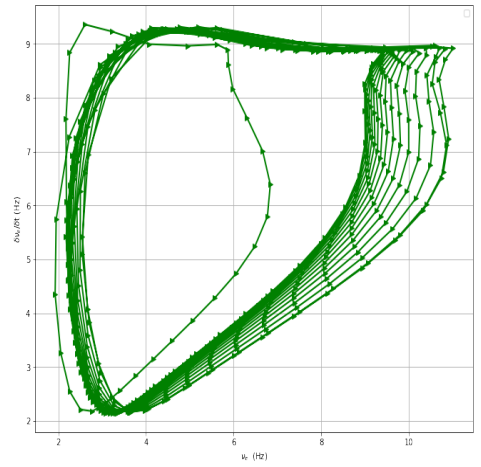

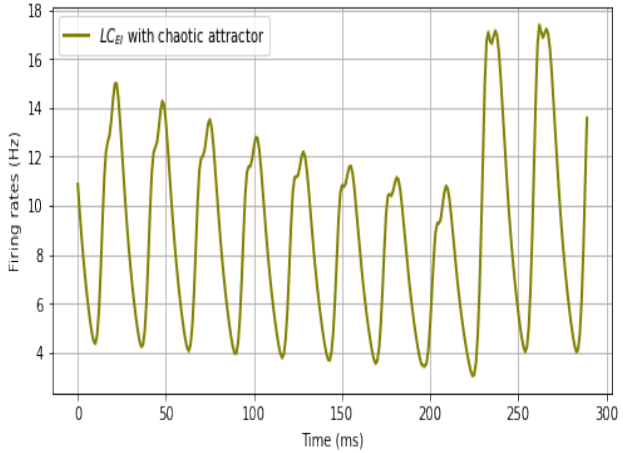

Simulation results

State 5 : Chaotic-like $State_2$

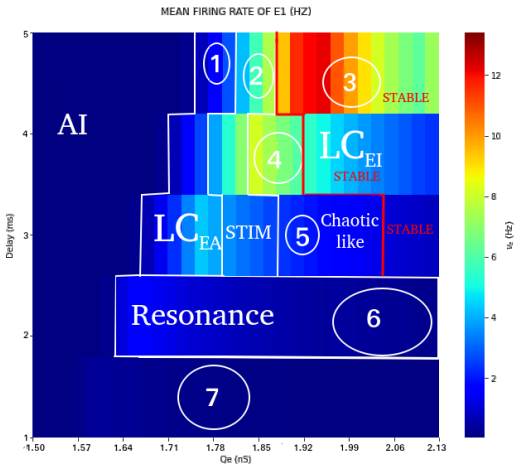

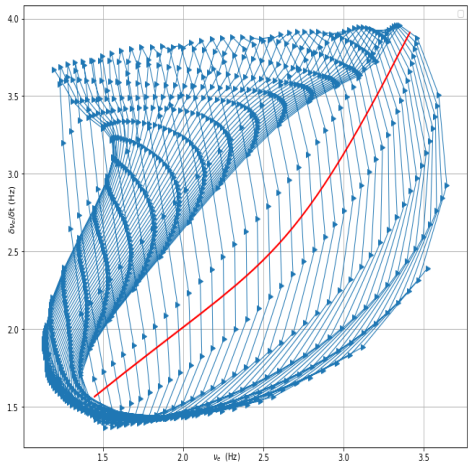

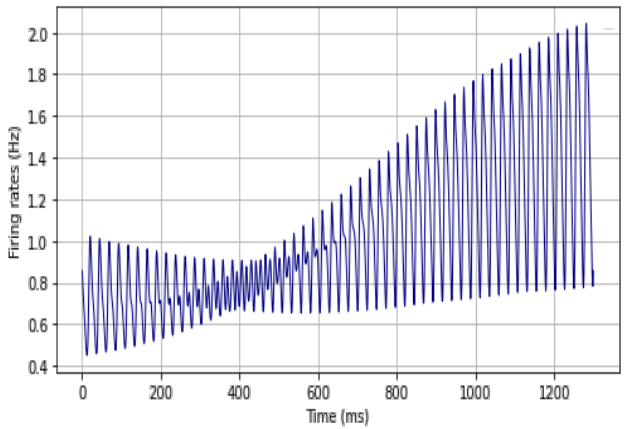

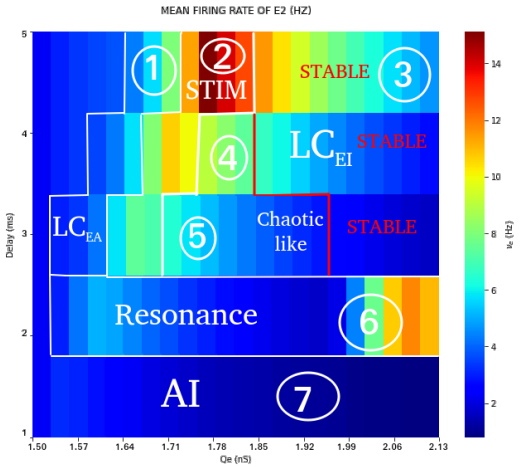

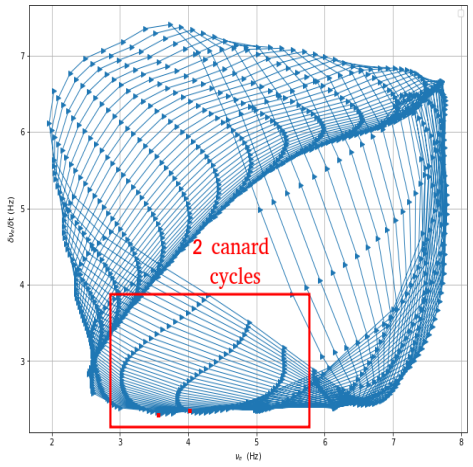

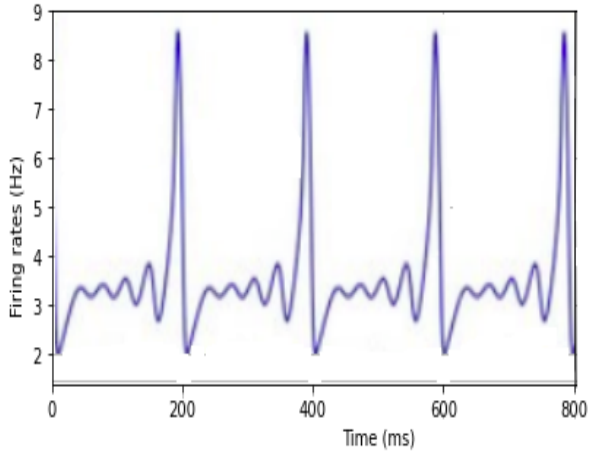

4 Simulations

Simulation results

	State 6: Resonance	State 7 : AI
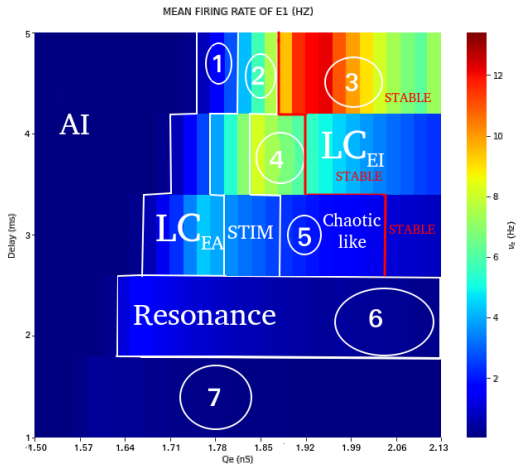	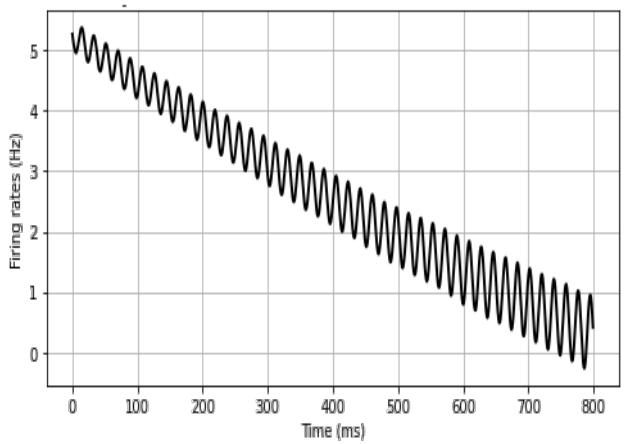	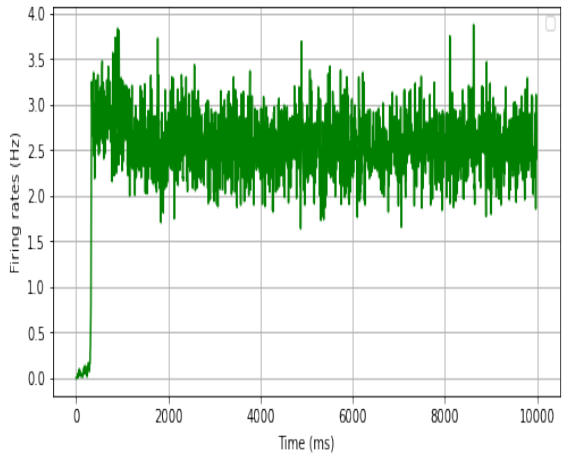
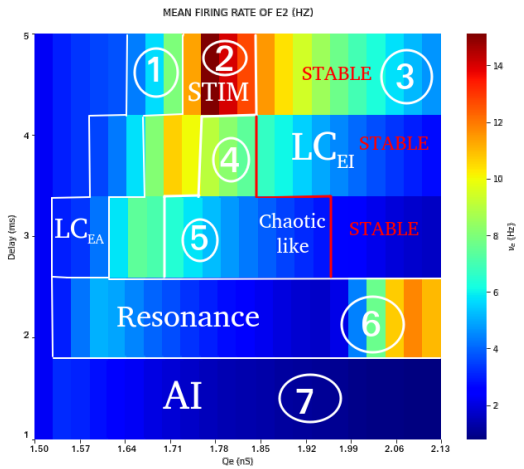	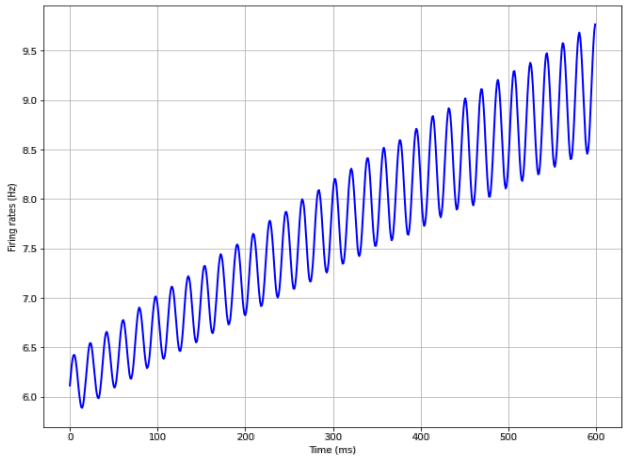	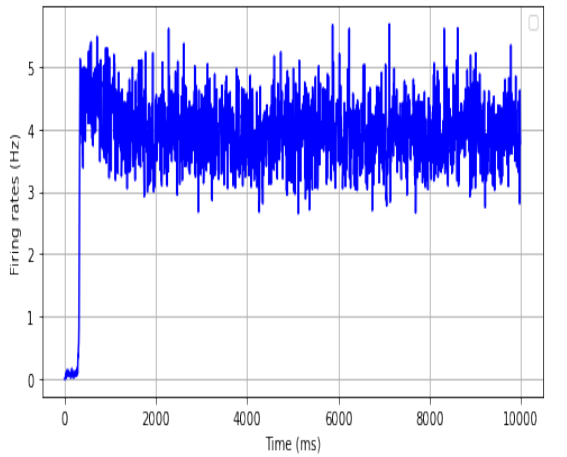

4 Simulations

Population I1& I2

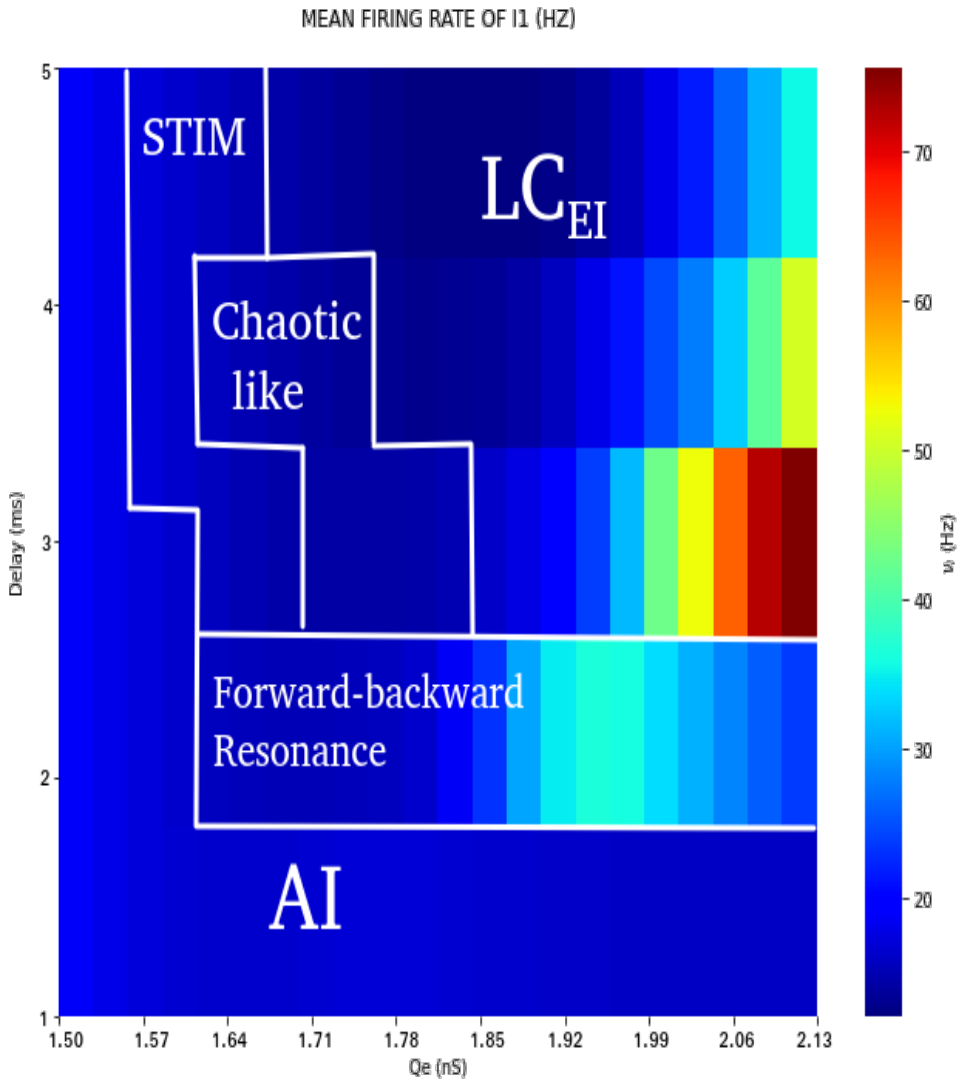

Figure 17: Bifurcation map of I1 states

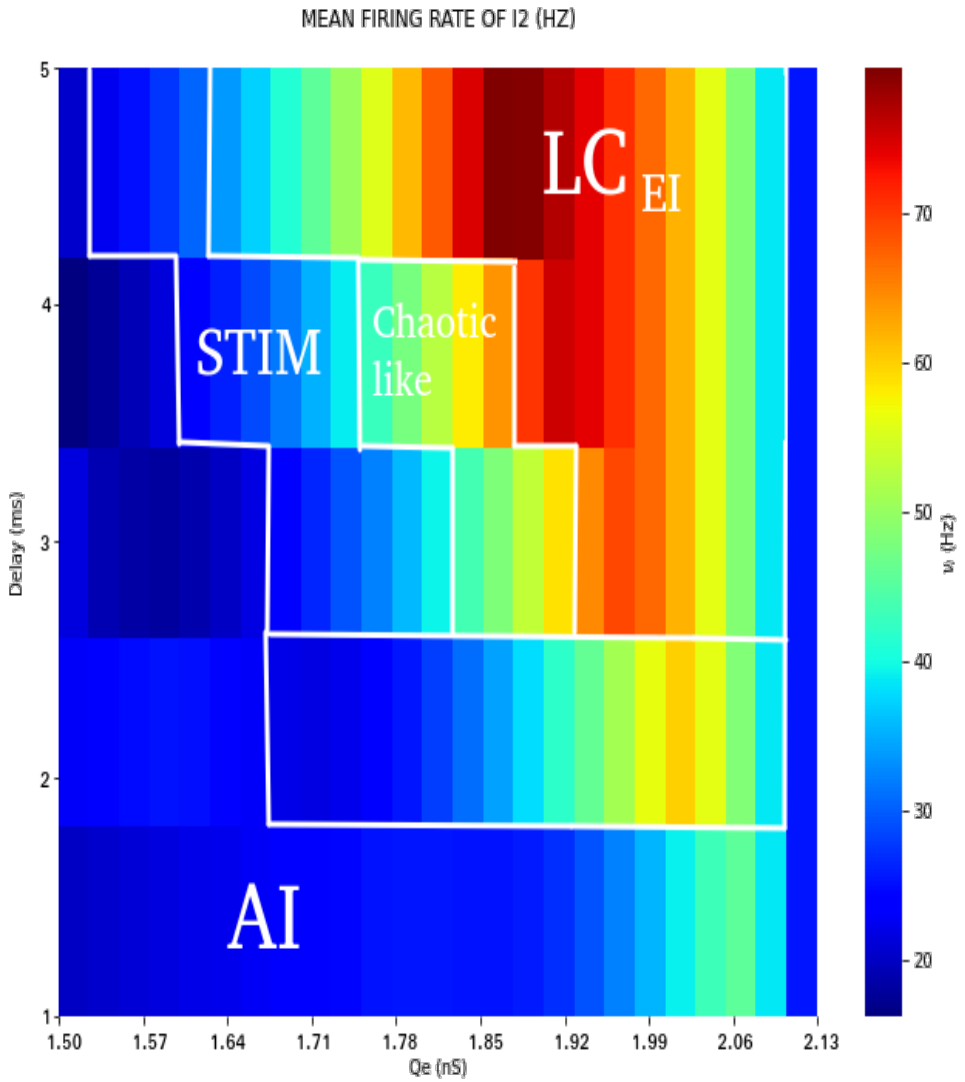

Figure 18: Bifurcation map of I2 states

5 Discussions

Table of contents

Results Outcomes

The outcomes of this study are the following ones

- Mean-field simulate AI states well
- High delays and $Q_e \Longrightarrow$ stabilisation of the system with LC_{EI}

	Delay (ms)	g=$\frac{Q_i}{Q_e}$ (nS)
E1	5	2.75
	4	2.6
	3	2.43
E2	5	2.7
	4	2.7
	3	2.56

	Delay (ms)	g=$\frac{Q_i}{Q_e}$ (nS)
I1	5	2.99
	4	2.84
	3	2.7
I2	5	3.05
	4	2.65
	3	2.65

- Mean input μ_{nu_α} impact $\Longrightarrow$ dominant inhibition phenomenon is delay dependent
- Unexpected behavior : LC_{EA} and θ-resonance

Model Limitations

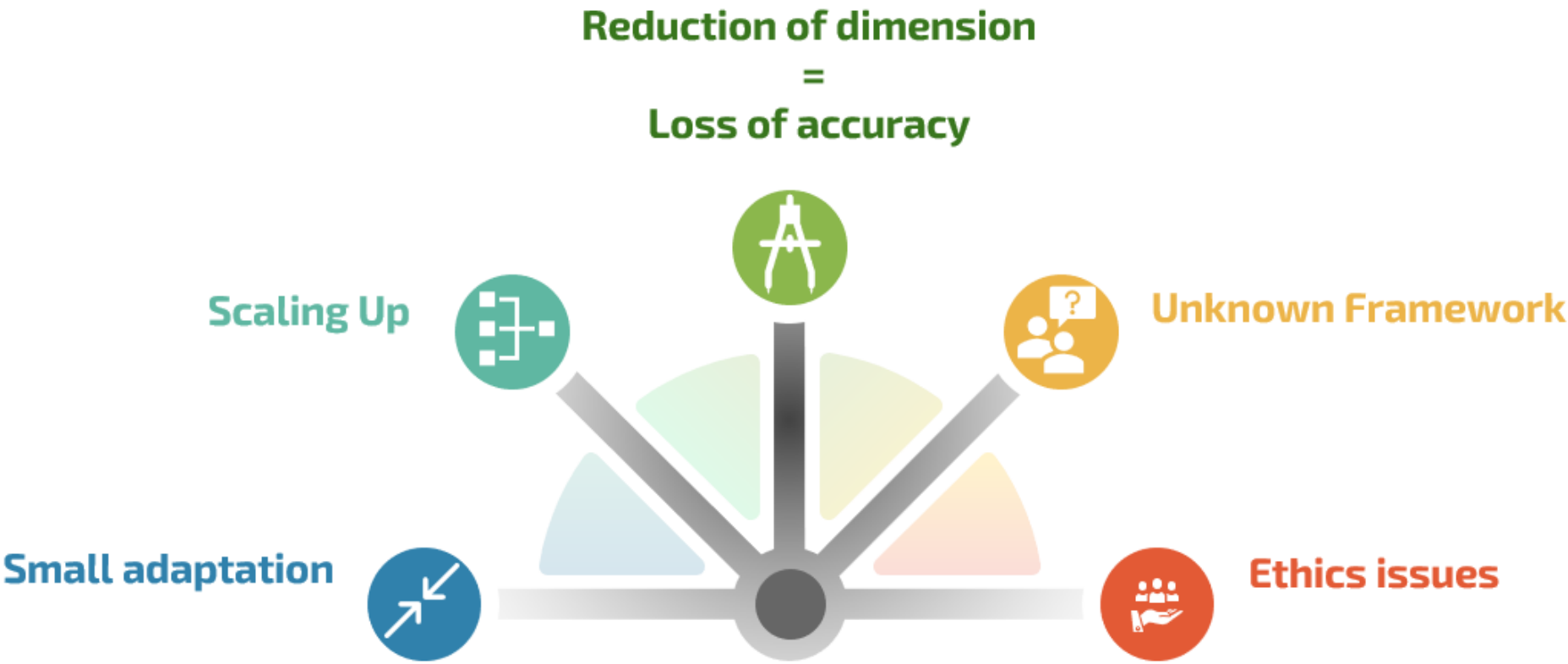

Figure 19: Obvious and Underlying Limits

Presentation ending

6 References

Table of contents

6 References

References I

[1] J. S. Goldman, L. Kusch, B. H. Yalcinkaya, D. Depannemaecker, T.-A. E. Nghiem, V. Jirsa, and A. Destexhe, "Brain-scale emergence of slow-wave synchrony and highly responsive asynchronous states based on biologically realistic population models simulated in the virtual brain," *bioRxiv*, 2020.

[2] P. Dayan and L. Abbott, *Theoretical Neuroscience: Computational and Mathematical Modeling of Neural Systems*, vol. 15. 01 2001.

[3] A.-M. Oswald, B. Doiron, J. Rinzel, and A. Reyes, "Spatial profile and differential recruitment of gaba(b) modulate oscillatory activity in auditory cortex," *The Journal of neuroscience : the official journal of the Society for Neuroscience*, vol. 29, pp. 10321–34, 08 2009.

[4] Y. Zerlaut, S. Chemla, F. Chavane, and A. Destexhe, "Modeling mesoscopic cortical dynamics using a mean-field model of conductance-based networks of adaptive exponential integrate-and-fire neurons," *Journal of Computational Neuroscience*, vol. 44, pp. 45–61, Feb. 2018.

[5] A. Rocha, "Toward a comprehensive understanding of eeg and its analyses," *SSRN Electronic Journal*, 01 2018.